J Fluoresc (2015) 25:1363–1369
DOI 10.1007/s10895-015-1626-x

ORIGINAL ARTICLE

Expression of Genes Involved in Porphyrin Biosynthesis Pathway in the Human Renal Cell Carcinoma

Hugo Nóbrega da Rocha Filho [1,2] · Evelin Caroline da Silva [1] · Flávia R. O. Silva [3] · Lilia Coronato Courrol [4] · Carlos Henrique de Mesquita [5] · Maria Helena Bellini [1,2]

Received: 13 April 2015 / Accepted: 26 July 2015 / Published online: 6 August 2015

Abstract Renal cell carcinoma (RCC) remains one of the greatest challenges of urological oncology and is the third leading cause of death in genitourinary cancers. Surgery may be curative when patients present with localized disease. Our previous results demonstrated the autofluorescence of blood PpIX in primary RCC mouse model and an increase in fluorescence intensity as a function of growth of the subcutaneous tumor mass. In another work, a nice correlation between the growth of the tumor mass and tissue fluorescence intensity was found. The aim of this study was to evaluate the expression profile of porphyrin biosynthesis pathway-related genes of human kidney cells. We used two kidney cell lines, one normal (HK2) and another malignant (Caki-1). Endogenous and 5-aminolevolinic acid (ALA) induced protoporphyrin IX (PpIX) HK2 and Caki-1 cells were analyzed by fluorescence spectroscopy. Real-time quantitative polymerase chain reaction (qRT-PCR) was used to measure mRNA of those genes. Emission spectra were obtained by exciting the samples at 405 nm. For ALA untreated cells the maximum fluorescence intensity was detected at 635 nm. The mean peak area of emission spectra in both cells types increased linearly in function of cell number. Besides, basal levels of PpIX autofluorescence of each cell concentration of HK2 samples were significantly lower than those of Caki-1 samples. For ALA-treated cells the mean PpIX spectra shows PpIX emission peak at 635 nm with a shoulder at 700 nm. Analysis of PpIX fluorescence intensity ratio between tumor cells and HK2 cells showed that fluorescence intensity was, on average, 26 times greater in tumor cells than in healthy cells. qRT-PCR revealed that in Caki-1 ALA-treated cells, PEPT gene was significantly up-regulated and FECH and HO-1 genes were significantly down regulated in comparison with HK2 ALA-treated cells. In conclusion, our results demonstrate the preferential accumulation of ALA-induced PpIX in human RCC and also indicate that PEPT1, FECH and HO-1 genes are major contributors to this accumulation.

Keywords Renal cell carcinoma · PpIX · Fluorescence · HK2 cells · Caki-1 cells · Porphyrin pathway

Introduction

Renal cell carcinoma (RCC) is the most common type of kidney cancer in adults and during the past two decades, the incidence of RCC has increased by approximately 2 % per year [1]. Kidney Clear cell RCC, the most common RCC tumor, arises from the proximal tubular epithelial cells (PTEC) [2]. The malignization process of PTEC is resulted of accumulation of mutations in the cells that cause alterations in the proteins functions and in the intracellular signaling pathways. These intracellular transformations contribute to tumor resistance to chemotherapy or radiotherapy. This, in fact, represents a challenge to the development of therapies.

Surgery may be curative when patients present with localized disease. However, the aggressive nature of RCC leads to

✉ Maria Helena Bellini
mhmarumo@terra.com.br

[1] Centro de Biotecnologia, IPEN/CNEN-SP, São Paulo, Brazil

[2] Disciplina de Nefrologia, Departamento de Medicina, UNIFESP, São Paulo, Brazil

[3] Centro de Ciência e Tecnologia dos Materiais, IPEN/CNEN-SP, São Paulo, Brazil

[4] Departamento de Ciências Exatas e da Terra, UNIFESP, São Paulo, Brazil

[5] Centro de Tecnologia das Radiações, IPEN-CNEN-SP, São Paulo, Brazil

recurrence and prognosis in these cases is poor. In fact, among patients choosing excision of a localized RCC, approximately 20 to 40 % will subsequently develop metastatic disease [3, 4]. Extent of resection is accepted as critical to optimal surgical treatment and patient prognosis.

Fluorescence spectroscopy is currently one of the most widely used spectroscopic techniques in the fields of biochemistry and molecular biophysics. Natural tissue fluorophores such as NAD-(P)H and FAD, structural proteins such as collagen, elastin, and their crosslinks, and the aromatic amino acids tryptophan, tyrosine, phenylalanine and porphyrins display characteristic excitation wavelengths with an associated characteristic emission [5, 6]. Biophysical changes that accompany malignant transformation process often lead to alterations in the optical characteristics of tissues. Optical technologies sensitive to these alterations can lead to the development of quantitative, noninvasive, real-time diagnostic tools [7].

Protoporphyrin, a porphyrin derivative, is the intermediate metabolic precursor of the heme molecule. The insertion of ferrous iron into protoporphyrin IX (catalyzed by the enzyme ferrochelatase) is the last step in heme biosynthesis that is properly called porphyrin biosynthesis. Protoporphyrin IX (PpIX) accumulates in cancerous tissues because of tumor-specific metabolic alterations. Several studies have been

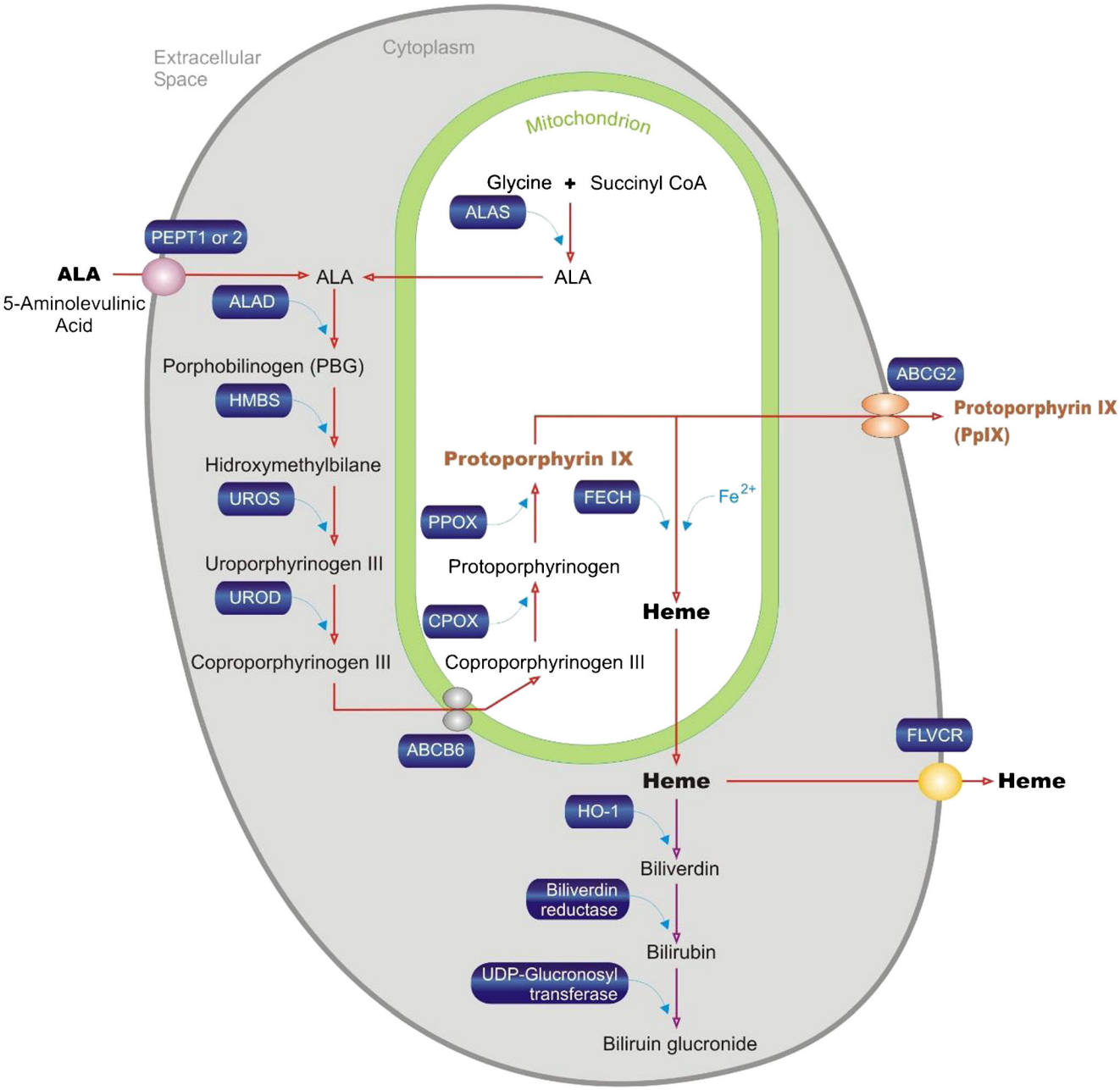

Fig. 1 Porphyrin bioynthesis pathway-related genes

performed to define the potential of autofluorescence for cancer diagnosis and treatment [8–10].

5-Aminolaevulinic acid (ALA) is a non-fluorescent amino acid derivative that is metabolized to PpIX via porphyrin biosynthesis pathway of biological systems. This pathway involves multiple enzymatic steps in the mitochondrion and in the cytosol of the cell and is regulated by a feedback control system and PpIX does not accumulate [11–15] (Fig. 1). However, in pathological conditions such as cancer, PpIX accumulates in intracellular compartments by avoiding this feedback control in the pathway of heme biosynthesis [16]. ALA is widely used to fluorescence-guide resection of solid tumors and in photodynamic therapy (PDT) [17].

In a previous study [8], our group demonstrated the autofluorescence of blood PpIX in primary RCC mouse model and an increase in fluorescence intensity at ~ 635 nm as a function of growth of the subcutaneous tumor mass. In another work, tumor-bearing kidneys in different progression stages were analyzed by ex-vivo spectroscopy, and a nice correlation between the growth of the tumor mass and fluorescence intensity was found [9]. Additionally, we demonstrated that the blood PpIX was positively correlated with metastatic nodule area vascularization, indicating that fluorescence spectroscopy could be useful as a biomarker for antiangiogenic cancer therapy [18]. The aim of this work was to evaluate gene expression modulation of enzymes and transporters involved in the porphyrin biosynthesis pathway in order to elucidate the molecular mechanisms of PpIX accumulation in human RCC.

Materials and Methods

Reagents

5-ALA was purchased from Sigma (St. Louis, MO, USA). For each cell experiment, ALA was freshly dissolved in phosphate-buffered saline (PBS). After the pH was adjusted to 7.4 and solutions were sterilized by filtration using a 0.2 μm pore filter and used at a final concentration of 50 μg per ml in serum free medium.

Cell Lines

HK2 is a proximal tubular epithelial cell (PTEC) line derived from normal kidney human (American Type Culture Collection, Manassas, VA). The cells were cultured Dulbecco's Modified Eagle Medium (DMEM): Nutrient Mixture F12 (Ham's) (3:1), supplemented with 100 U/mL penicillin, 50 mg/mL streptomycin, and 10 % fetal bovine (Life Technologies, Grand Island, NY).

Caki-1 is a human malignant tubular epithelial cell line (ATCC® HTB-46™) were grown in McCoy's medium with L-Glutamine, supplemented with 10 % fetal bovine serum, 10 mM HEPES buffer, 100U/ml penicillin, and 100 mg/ml streptomycin. (Life Technologies, Grand Island, NY).

Both cell lines were maintained in a chamber at 37 °C in an atmosphere containing 5 % CO2, 37 °C and 95 % humidity.

PpIX Accumulation in Cells

Both HK2 and Caki-1 cells were divided in two groups, incubated with and without ALA. The cells incubated with ALA were cultivated in 175 cm^2 flasks in serum free medium. Before the experiments, the medium was replaced with 10 mL fresh serum free medium containing ALA (50 μg/mL) [19]. After 4 h the cells were washed with PBS and detached by the addition of 0.25 % trypsin. Afterwards cell viability was assessed using Trypan Blue exclusion method. Cell suspensions were subdivided into three equal aliquots in the quantity

Table 1 Primer sequences for real-time RT-PCR

Gene		Primer sequence
PEPT1	Foward	TCTTCTCTGTCACGGGATTGG
	Reverse	GCACCGACTTCATGTTGGAA
PEPT2	Foward	AAAGAAGCCATCTCCGACAATC
	Reverse	CACCACAATGAAGGCAATGC
ALAD	Foward	TCCAACCTCATCTACCCCATCT
	Reverse	GAGGCTGGTGATAGGCTGTATGT
HMBS	Foward	CCTGCCCACTGTGCTTCCT
	Reverse	GGTTTTCCCGCTTGCAGAT
UROS	Foward	TCAGCACTGCCTCTTCTATTTCC
	Reverse	GAGCGCTTTTGGCAGGATT
UROD	Foward	GGGCAGTTGGTGAAGCAGAT
	Reverse	GGCCCAGGTTGGCAATG
ABCB6	Foward	CAGCAGGGACAGGAAGAAACC
	Reverse	CTTTTGTCACCGTTCCATGGT
CPOX	Foward	AGGGACTGGGTGCGTTGAT
	Reverse	ATCGTGTGCCCTCCAAACC
PPOX	Foward	GGGCAAAGAGCCTGATGAGA
	Reverse	ACGCCACCTCAGGTCCAA
ABCG2	Foward	GGCTTTGCAGCATAATGAATTTTT
	Reverse	TACAAGGATTGTTTCCTGTTGCAT
FECH	Foward	GCAGGTGGTGCCCTTCAG
	Reverse	TACTCTTTGGCAAGATGCATCAG
HO-1	Foward	TCCGATGGGTCCTTACACTCA
	Reverse	TCACATGGCATAAAGCCCTACA
FLVCR	Foward	TCGCTGGTCAACGCCTTT
	Reverse	GCAGCAAGGTGACACCGTAGA
ALAS-1	Foward	GATGCCAGGCTGTGAGATTTACT
	Reverse	CGAATCCCTTGGATCATGGA
GAPDH	Foward	CACATGGCCTCCAAGGAGTAA
	Reverse	TGAGGGTCTCTCTCTTCCTCTTGT

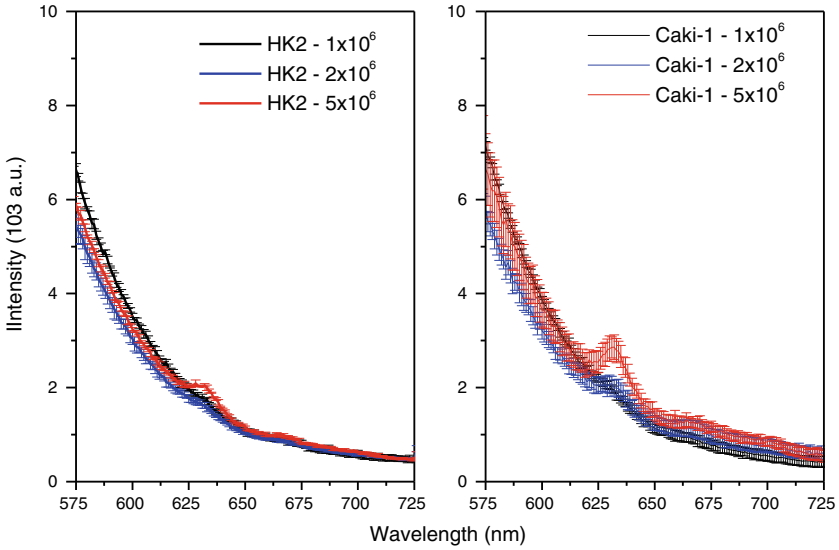

Fig. 2 Mean emission spectra of PpIX extracted from Hk2 and Caki-1 cells in the wavelength range of 575–725 nm in three different cell number (1×10^6, 2×10^6 and 5×10^6 cells)

of 1×10^6, 2×10^6, and 5×10^6 cells. Cells were pelleted by centrifugation (5000 rpm /5 min) and the pellets were processed to quantitate PpIX. All the experiments were done in triplet.

PpIX Extraction

To each cell pellet 1 mL of analytical-grade acetone was added and thoroughly mixed. The mixture was then centrifuged at 4000 rpm for 15 min. The clear supernatant was transferred to a clean tube and maintained at 4 °C, protected from light, until spectrofluorimetric analysis.

Flourescent Spectral Analyses

The emission spectra of the samples from the in vitro assay were analyzed with a 1-mm path length and studied on a Jobin Yvon (Longjumeau, France) Fluorolog-3 spectrometer with front-face collection geometry and a 0.2-nm resolution. The *bandwidth* for emission was 2 nm.

RNA Extraction and cDNA Synthesis

Total RNA was extracted from 5×10^6 cells using Trizol reagent (Invitrogen, Carlsbad, CA) according to the manufacturer's instruction. Total cellular RNA was eluted in 35 μl DEPC-treated H_2O (Invitrogen®), quantified on a Nanodrop® spectrophotometer (ND-100, Thermo Fisher Scientific Inc. Waltham, MA, USA) after which samples were stored at -80 °C until analysis.

cDNAs were synthesized from 2 μg of total RNA by the addition of 2 μg of oligodT (Invitrogen®), 8 μl 5× FS buffer (Invitrogen®), 2 μl dNTP (10 mM), 2 μl DTT (0.1 M, Invitrogen®), 2 μl RNAseOUT (40 U/μl, Invitrogen®) and 2 μl M-MLV (200 U/μl, Invitrogen®). The final 40 μl reaction mixture was incubated at 20 °C for 10 min, 42 °C for 45 min and 95 °C for 5 min. The Synthesized cDNAs were stored at −20 °C for further expression analysis.

Table 2 Mean area of emission spectra of PpIX extracted from Hk2 and Caki-1 cell lines in the wavelength range of 575—725 nm

Cell number	HK2	Caki-1	*P*
1×10^6	10,160±2713	22,090±8,454	<0.05
2×10^6	18,838±5468	40,326±4,074	<0.01
5×10^6	56,991±2878	140,000±10,721	<0.01

qRT-PCR

qRT-PCR was performed to measure the expression of Peptide transporter 1 (PEPT1), Peptide transporter 2 (PEPT2), Delta-

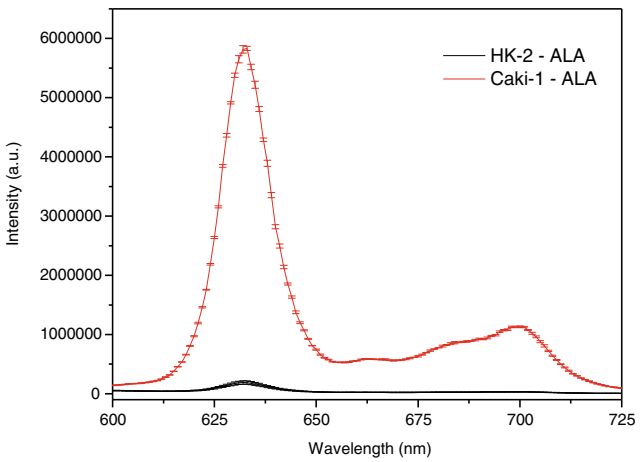

Fig. 3 Mean emission spectra of PpIX extracted from Hk2 and Caki-1 cells (5×10^6) incubated with 50 μg of ALA for 4 h

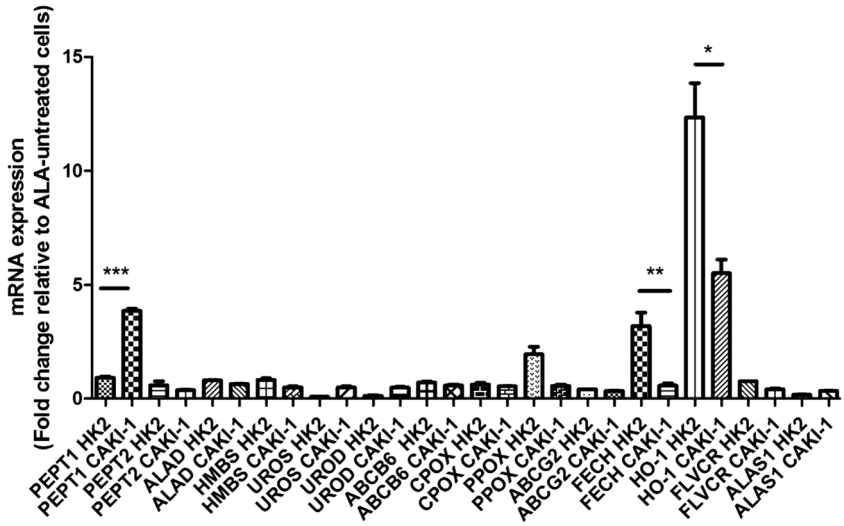

Fig. 4 Expression of PEPT1, PEPT2, ALAD, HMBS, UROS, UROD, ABCB6, CPOX, PPOX, ABCG2, FECH, HO-1, FLVCR and ALAS1 genes in HK2 and Caki-1 cells after 4-h incubation with 50ug of ALA. *$P<0.05$; **$P<0.01$; ***$P<0.001$. Student's *t-test*

aminolevulinic acid dehydratase (ALAD), Hydroxymethylbilane synthase (HMBS), Uroporphyrinogen III synthase (UROS), Uroporphyrinogen III decarboxylase (UROD), ATP-binding cassete, subfamily C (ABCB6), Coproporphyrinogen oxidase (CPOX), Protoporphyrinogen oxidase (PPOX), ATP-binding cassette, sub-family G, member 2 (ABCG2), Ferrochelatase (FECH), Heme oxygenase-1 (HO-1), Feline leukemia virus sub-group C receptor (FLVCR), 5-aminolevulinatesynthase-1 (ALAS1). Glyceraldehyde-3-phosphate dehydrogenase (GAPDH) was used as housekeeping gene. The sequences of primers used for qRT-PCR are listed in Table 1. Amplification was carried out by real-time PCR (7300 System, Applied Biosystems®) as follows: denaturation at 94 °C for 1 min, annealing at 60 °C for 1 min, and extension at 72 °C for 1 min.

The statistical analysis of the qRT-PCR results was performed using the ΔCt value ($Ct_{gene\ of\ interest}$-$Ct_{calibrator}$). Relative gene expression was calculated according to the ΔΔCt method (ΔCt_{sample}-ΔCt_{GAPDH}) using the control group as a reference for comparison. To convert between ΔΔCt and relative gene expression levels, the fold change was calculated using the following equation: $2^{-\Delta\Delta Ct}$.

Statistical Analysis

The results are presented as means ± SE. Comparisons between groups were performed by Student's *t* test. The difference between groups was considered statistically significant when probability was equal or less than 0.05.

Results and Discussion

The survival rates in patients that were treated with partial or radical nephrectomy depends on the complete removal of tumor cells. Therefore, the development of new treatments tools are very important to management of RCC.

In this work we performed in vitro experiments with cell lines derived from normal (HK2 cells) and tumor human tissue (Caki-1 cells).

In all experiments, cell viability was never below 95 % in both cell lines.

Initially fluorescence spectroscopy was used to estimate intracellular basal levels of PpIX in the Hk2 and Caki-1 cell lines. PpIX was evaluated in samples consisting of three different cell number (1×10^6, 2×10^6 and 5×10^6 cells) that were excited at 420 nm, and emission was collected between 575 and 725 nm. The spectral curves for the normal and cancerous cells are displayed in Fig. 2 where it can be noticed a light scattering attributed to the long wavelength tails of short wavelength emitting fluorophores, such as proteins, NAD(P)H, fatty acids, vitamin A, and lipopigments [20]. Moreover, an emission peak at 635 nm was observed. This peak in the red is assumed to be predominantly caused by PpIX [8, 9]. It can be seen that the mean peak area of emission spectra in both cells types increases linearly as a function of cell number. Besides, basal levels of PpIX autofluorescence of each cell concentration of HK2 samples were significantly lower than that of Caki-1 samples. (Table 2) These data indicated that kidney tumor cells have altered regulation of heme metabolism. Then, the next step was to verify the accumulation of PpIX in these cell types after ALA treatment.

The fluorescence spectra recorded in the range 575–725 nm, for the normal and cancerous cells under excitation at 405 nm show the light scattering from the shorter wavelength fluorescence.

Intracellular accumulation of PpIX was quantified in HK2 and Caki-1 cell lines after ALA treatment for 4 h in serum free medium [18]. PpIX spectra shows PpIX emission peak at 635 nm with a shoulder at 700 nm. (Fig. 3) Mean emission

peak area was 3.78E6±7.45E5 nm for HK2-ALA cells and 1.00E8±1.19E6 nm for Caki-1-ALA cells. So that, ALA-induced PpIX accumulation was approximately 26 times higher in RCC than normal cells. This finding corroborates our previous in vivo results, showing a good correlation between emission band intensity at 635 nm and the size of the tumor area [9].

The preferential accumulation of PpIX in tumor cells has been found in many kinds of malignant cells [21–23]. However, the mechanism of preferential accumulation of PpIX in these cells remains obscure. To elucidate the mechanisms of PpIX accumulation in the Caki-1 cells, the expression of relevant enzymes of the porphyrin pathway was studied by RT-qPCR. To determine the differentially expressed genes a fixed fold-change cut-off (2-fold) was used [24].

figure 4 shows the mRNA expression levels of HK2 and Caki-1 ALA-treated cells. PEPT1 mRNA levels were significantly higher in Caki-1 cells than in HK2 cells (3.9-fold, $P<0.0001$) which suggests that this H^+-coupled oligopeptide transporter plays an important role in the transporter system for the uptake of ALA into human RCC cells. The expression of this ALA influx transporter has been found in a variety of human cancer such as bladder, pancreatic and gastric [25, 26].

mRNA levels FECH and HO-1 genes were significantly lower in Caki- cells than in HK2 cells. (Fig. 4) Decreased mRNA levels of these enzymes can be correlated with large amounts of PpIX found in Caki-1 cells. The transition from PpIX to heme is controlled by FECH activity and down-regulation or loss of enzymatic activity correspond with an enhanced PpIX fluorescence [27]. Finally, it is known that HO-1 catalyzes degradation of PpIX via heme pathway. Low levels of HO-1 lead to an increased amount of intracellular PpIX [28].

Conclusion

To the best of our knowledge, this is the first report that describes the expression profile of porphyrin biosynthesis pathway-related genes of a human RCC cell line. PEPT1, FECH and HO-1 genes are major contributors to RCC PpIX accumulation.

Acknowledgments This study was supported by FAPESP (Process number: 2010/52180-4) and CNPq (Process number: 134303/2013-0)

References

1. Jorge A, Garcia MD, Brian I, Rini MD (2007) Recent progress in the management of advanced renal cell carcinoma. CA Cancer J Clin 57:112–125
2. Morais C, Johnson DW, Vesey DA, Gobe GC (2013) Functional significance of erythropoietin in renal cell carcinoma. BMC Cancer 13:14
3. Hollingsworth JM, Miller DC, Daignault S, Hollenbeck BK (2007) Five-year survival after surgical treatment for kidney cancer: a population–based competing risk analysis. Cancer 109:1763–1768
4. Assouad J, Petcova B, Berna P, Dujon A, Foucault C, Riquet M (2007) Renal cell carcinoma metastases surgery: pathologic findings and prognostic factors. Ann Thorac Surg 84(4):1114–1120
5. Schantz SP, Savage HE, Sacks P, Alfano RR (1997) Native cellular fluorescence and its application to cancer prevention. Environ Health Perspect 105(4):941
6. Ramanujam N (2000) Fluorescence spectroscopy of neoplastic and non-neoplastic tissues. Neoplasia 2(1–2):89–117
7. Chang KS, Ina P, Marin N, Follen M, Richards-Kortum R (2005) Fluorescence spectroscopy as a diagnostic tool for detecting cervical pre-cancer. Gynecol Oncol 99:S61–S63
8. Courrol LC, Silva FRO, Coutinho EL, Piccoli MF, Mansano RD, Vieira ND, Schor N, Bellini MH (2007) Study of blood porphyrin spectral profile for diagnosis of tumor progression. J Fluoresc 17(3):289–292
9. Bellini MH, Coutinho EL, Courrol LC, Silva FRO, Vieira ND, Schor N (2008) Correlation between autofluorescence intensity and tumor area in mice bearing renal cell carcinoma. J Fluoresc 18(6):1163–1168
10. Kusunoki Y, Imamura F, Uda H, Mano M, Horai T (2000) Early detection of lung cancer with laser-induced fluorescence endoscopy and spectrofluorometry. Chest 118:1776–1782
11. Tsai TM, Hong RL, Tsai JC (2004) Effect of 5-aminolevulinic acid-mediated photodynamic therapy on MCF-7 and MCF-7/ADR cells. Lasers Surg Med 34:64–72
12. Heyerdahl H, Wang I, Liu DL, Berg R, Andersson-Engels S, Peng Q, Moan J, Svanberg S, Svanberg K (1997) Pharmacokinetic studies on 5-aminolevulinic acid-induced protoporphyrin IX, accumulation in tumors and normal tissues. Cancer Lett 112:225–231
13. Van Der Breggen EWJ, Rem AI, Cristian MM, Yang CJ, Calhoun KH, Sterenborg HJCM, Motamedi M (1996) Spectroscopic detection of oral and skin tissue transformation in a model for squamous cell carcinoma: autofluorescence versus systemic aminolevulinic acid-induced fluorescence. IEEE J Sel Top Quantum Electron 2: 997–1007
14. Moesta KT, Ebert B, Handke T, Nolte D, Nowak C, Haensch WE, Pandey RK, Dougherty TJ, Rinneberg H, Schlag PM (2001) Protoporphyrin IX occurs naturally in colorectal cancers and their metastases. Cancer Res 61:991–999
15. Tsuji T, Sasaki Y, Tanaka M, Hanabata N, Hada R, Munakata A (2002) Microvessel morphology and vascular endothelial growth factor expression in human colonic carcinoma with or without metastasis. Lab Investig 82:555–562
16. Otake M, Nishiwaki M, Kobayashi Y, Baba S, Kohno E, Kawasaki T, Fujise Y, Nakamur H (2003) Selective accumulation of ALA-induced PpIX and photodynamic effect in chemically induced hepatocellular carcinoma. Br J Cancer 89:730–736
17. Bourré L, Giuntini F, Eggleston IM, Wilson M, MacRobert AJ (2008) 5-Aminolaevulinic acid peptide prodrugs enhance photosensitization for photodynamic therapy. Mol Cancer Ther 7:1720–1729
18. Rocha FGG, Chaves KCB, Gomes CZ, Campanharo CB, Courrol LC, Schor N, Bellini MH (2010) Erythrocyte protoporphyrin fluorescence as a biomarker for monitoring antiangiogenic cancer therapy. J Fluoresc 20:1225–1231
19. Chakrabarti P, Orihuela E, Egger N, Neal DE Jr, Gangula R, Adesokun A, Motamedi M (1998) Delta-aminolevulinic acid-

mediated photosensitization of prostate cell lines: implication for photodynamic. Ther Prostate Cancer Prostate 36:211–218
20. Croce AC, Santamaria G, De Simone U, Lucchini F, Freitas I, Bottiroli G (2011) Naturally-occurring porphyrins in a spontaneous-tumour bearing mouse model. Photochem Photobiol Sci 10:1189–1195
21. Millon SR, Ostrander JH, Yazdanfar S, Brown JQ, Bender JE, Rajeha A, Ramanujam N (2010) Preferential accumulation of 5-aminolevulinic acid-induced protoporphyrin IX in breast cancer: a comprehensive study on six breast cell lines with varying phenotypes. J Biomed Opt 15:018002- 1–018002- 8
22. Smits T, Robles CA, van EP EJ, van de Kerkhof PCM, Gerritsen MJ P (2005) Correlation between macroscopic fluorescence and protoporphyrin IX content in psoriasis and actinic keratosis following application of aminolevulinic acid. J Investig Dermatol 125: 833–839
23. Silva FRO, Bellini MH, Nabeshima CT, Schor N, Vieira ND Jr, Courrol LC (2011) Enhancement of blood porphyrin emission intensity with aminolevulinic acid administration: a new concept for photodynamic diagnosis of early prostate cancer. Photodiagnosis Photodynamic Ther 8:7–13
24. Bigler J, Rand HA, Kerkof K, Timour M, Russell CB (2013) Cross-study homogeneity of psoriasis gene expression in skin across a large expression range. PLoS ONE 8:e52242
25. Nakanishi T (2007) Drug transporters as targets for cancer chemotherapy. Cancer Genomics Proteomics 4:241–254
26. Hagiya Y, Fukuhara H, Matsumoto K, Endo Y, Nakajima M, Tanaka T, Okura I, Kurabayashi A, Furihata M, Inoue K, Shuin T, Ogura S (2013) Expression levels of PEPT1 and ABCG2 play key roles in 5-aminolevulinic acid (ALA)-induced tumor-specific protoporphyrin IX (PpIX) accumulation in bladder cancer. Photodiagnosis Photodynamic Ther 10: 288–295
27. Kemmner W, Wan K, Rüttinger S, Ebert B, Macdonald R, Klamm U, Moesta KT (2008) Silencing of human ferrochelatase causes abundant protoporphyrin-IX accumulation in colon câncer. FASEB J 22:500–509
28. Nowis D, Legat M, Grzela T, Niderla J, Wilczek E, Wilczynski GM, Glodkowska EG, Mrowka P, Issat T, Dulak J, Jozkowicz A, Was H, Adamek M, Wrzosek A, Nazarewski S, Makowski M, Stokosa T, Jako bisiak M, Goab J (2006) Heme oxygenase-1 protects tumor cells against photodynamic therapy-mediated cytotoxicity. Oncogene 25:3365–3374